

Multiple Separatrix Crossing: A Chaos Structure[¶]

B. V. Chirikov* and V. V. Vecheslavov**

Budker Institute of Nuclear Physics, Siberian Branch, Russian Academy of Sciences, Novosibirsk, 630090 Russia

**e-mail: chirikov@inp.nsk.su*

***e-mail: vecheslavov@inp.nsk.su*

Received January 20, 2000

Abstract—Numerical experiments on the structure of the chaotic component of motion under multiple-crossing of the separatrix of a nonlinear resonance with a time-varying amplitude are described with the emphasis on the ergodicity problem. The results clearly demonstrate nonergodicity of this motion due to the presence of a regular component of a relatively small measure with a very complicated structure. A simple 2D-map per crossing is constructed that qualitatively describes the main properties of both chaotic and regular components of the motion. An empirical relation for the correlation-affected diffusion rate is found including a close vicinity of the chaos border where evidence of the critical structure is observed. Some unsolved problems and open questions are also discussed. © 2000 MAIK “Nauka/Interperiodica”.

1. INTRODUCTION

The present work continues the studies of chaotic motion under a slow separatrix crossing. This is a particular case of adiabatic processes that is very important in physics because of the adiabatic invariance, that is, of the conservation of action variables (J) under a slow parametric perturbation (even though this is only an approximate invariance). The main problem here is the degree of accuracy or of violation of the adiabatic invariance. Separatrix crossing produces the largest chaotic component in phase space whose size does not depend on the adiabatic parameter $\epsilon \rightarrow 0$ (which nevertheless affects the detailed structure of the motion and its time scale).

In our previous paper [1], the single separatrix crossing for a particular model was described in detail. Remarkably, a fairly simple relation, that we used for the model of [2], turned out to be surprisingly accurate within a large part of the chaotic component.

In this paper, we describe the results of numerical experiments on multiple separatrix crossing. We focus on statistical properties of the motion, including the structure and measure of the regular component disseminated into the chaotic “sea” in a rather tricky way. The existence of the regular component means nonergodicity of the motion, the question which has remained unclear for a long time up until recently. To our knowledge, the nonergodicity of motion in a similar model was first predicted theoretically and estimated numerically in [3]. We have confirmed this result by different methods and found many other characteristics of the motion structure. The present work, as well as the previous one [1], was stimulated by a very interesting study of the corresponding quantum adiabaticity [4]. We use the same classical model, which is briefly described,

for the reader’s convenience, in the next section (for details, see [1]).

2. THE MODEL AND TECHNIQUES

The model is determined by the Hamiltonian

$$H(x, p, t) = \frac{p^2}{2} + A_0 \sin(\Omega t) \cos x, \quad (2.1)$$

which describes a single nonlinear resonance in the pendulum approximation (see, e.g., [5, 6]) with a time-varying amplitude

$$A(t) = A_0 \sin(\Omega t). \quad (2.2)$$

The dimensionless adiabaticity parameter is defined in the usual way as the ratio of perturbation/oscillation where the tilde denotes the quantities rescaled by the frequencies,

$$\epsilon = \frac{\Omega}{\sqrt{A_0}}, \quad (2.3)$$

where $\sqrt{A_0}$ is a constant frequency of the small pendulum oscillation for the maximal amplitude.

Two branches of the instant, or “frozen”, separatrix at some $t = \text{const}$ are given by the relation

$$p_s(x'; t) = \pm 2\sqrt{|A(t)|} \sin\left(\frac{x'}{2}\right), \quad (2.4)$$
$$x' = \begin{cases} x, & A(t) > 0, \\ x - \pi, & A(t) < 0. \end{cases}$$

Following previous studies of the separatrix crossing, we restrict ourselves to this frozen approximation in

[¶]This article was submitted by the authors in English.

Regular component under separatrix crossing

n	ϵ	$\mu_r \times 10^2$	$T \times N_{tr}$	N_b
1	0.1	0.68 ± 0.2	$2 \times 10^3 \times 1000$	200
2	0.05	0.75 ± 0.06	$4 \times 10^5 \times 200$	500
3	0.033	0.70 ± 0.2	$4 \times 10^5 \times 200$	200
4	0.033	0.81 ± 0.08	$4 \times 10^5 \times 150$	500
5	0.02	0.60 ± 0.05	$2 \times 10^6 \times 100$	200
6	0.01	0.75 ± 0.04	$4 \times 10^6 \times 100$	200

Note: ϵ is the adiabaticity parameter; μ_r is the total relative measure of regular component; T is the number of separatrix crossings for each of the N_{tr} trajectories; N_b is the number of histogram bins in Fig. 1. n is the reference number for Fig. 1.

what follows. As shown in [1], the latter provides good accuracy of rather simple theoretical relations.

In this approximation, the action variable is defined in the standard way as

$$J = \frac{1}{2\pi} \oint p(x) dx, \tag{2.5}$$

where the integral is taken over the whole period for x rotation (off the resonance) and over a half of that for x oscillation (inside the resonance). This distinction is necessary to avoid the discontinuity of J at the separatrix where the action is given by a simple expression

$$J = J_s(t) = \frac{4}{\pi} \sqrt{|A(t)|} \leq J_{\max} = \frac{4}{\pi} \sqrt{A_0}. \tag{2.6}$$

At $\Omega t = 0 \pmod{\pi}$, the action is $J = |p|$, and the conjugated phase is $\theta = x$. Note that unlike p , the action $J \geq 0$ is never negative.

In what follows, we set $A_0 = 1$, and introduce the dimensionless action by the transformation $J/J_{\max} \rightarrow J$. The crossing region swept by the separatrix is then the unit interval, and J is simply related to the crossing time $t = t_{cr}$ by

$$|A(t_{cr})| = J^2, \quad 0 \leq J \leq 1, \tag{2.7}$$

while the adiabaticity parameter becomes $\epsilon = \Omega$.

Numerical integration of the equations of motion for Hamiltonian (2.1) was performed in (x, p) variables using two algorithms. In most cases, it was the so-called bilateral symplectic fourth-order Runge-Kutta algorithm as in [1]. However, in a few long runs, we applied a very simple first-order algorithm as in [2], which also is symplectic and which actually amounts to the well-known standard map [5] with the time-varying parameter

$$\bar{p} = \tilde{p} + \tilde{A}_0 \sin(\tilde{\Omega} \tilde{t}) \sin x, \quad \bar{x} = x + \tilde{p}, \tag{2.8}$$

where the tilde denotes the quantities rescaled by the transformation

$$\tilde{A}_0 = \frac{1}{s^2}, \quad \tilde{t} = st, \quad \tilde{\Omega} = \frac{\Omega}{s}, \quad \tilde{p} = \frac{p}{s}. \tag{2.9}$$

Here, s is the scaling parameter and we remind the reader that $A_0 = 1$. The primary goal of the rescaling was to decrease the parameter \tilde{A}_0 that controls the computation accuracy. Usually, it was around $\tilde{A}_0 \approx 0.1$.

As is well known, the variation of J under an adiabatic perturbation consists of two qualitatively different parts: (i) the average action, which is nearly constant between the crossings up to an exponentially small correction, and which is of primary interest in our problem, and (ii) the rapid oscillation with the motion frequency. The ratio of the two time scales is $\sim \epsilon / \sqrt{|A(t)|} \ll 1$, which allows one to efficiently suppress the second unimportant part of the J variation by simply averaging $J(t)$ over a long time interval $\sim 1/\epsilon$ (see [1]).

3. ERGODICITY

The ergodicity is the weakest statistical property in dynamical systems (see, e.g., [7]). Nevertheless, it is an important characteristic of the motion, necessary in statistical theory (see, e.g., [8]).

The question of ergodicity of the motion under the separatrix crossing remained open for a long time up until recently. The upper bound for the measure (the phase - space area) of a separate domain with the regular motion (a ‘‘stability islet’’) was estimated in [9] as $\mu_1 \leq \epsilon$.

To our knowledge, the nonergodicity of motion in a similar model was first predicted theoretically and estimated numerically in [3]. The authors directly calculated the number and positions of stable trajectories for two different periods. Moreover, they were able to locate some of these trajectories in the computation, thereby measuring their area in phase space (which turned out to be surprisingly small).

Here, we use a different, statistical, approach. To this end, we first obtain, from numerical experiments, the steady-state distribution $f_s(J)$ in the action. For the ergodic motion, it must be constant. Examples of the distribution are shown in Fig. 1 with the parameters listed in the table. The striking feature of all the distributions is a clear and rather specific inhomogeneity, reminiscent of a burst of icicles hanging down from a nearly ‘‘ergodic roof’’. This directly demonstrates the generic nonergodic character of motion under the separatrix crossing.

The histograms are normalized such that $f_s(J) = 1$ for the ergodic motion, and the sum over all the bins is also unity for any distribution. As a result, the dips in the distribution (‘‘icicles’’), indicating the regular component, are compensated by an increase in the ergodic background. The latter is clearly seen in all the distributions, especially for small J , and is a measure of the regular component. Namely, the relative measure (share) is given by the approximate relation

$$\mu_r \approx \langle f_s(J) - 1 \rangle, \quad J < J_1, \tag{3.1}$$

where J_1 is the position of the first dip from the bottom. The approximation comes from the border effects around $J = 1$ for any finite ϵ . Typically, at this theoretical border $f_s(1) \approx 0.5$, and drops to zero within the interval $|J - 1| \sim \epsilon$. For this reason, we also used other methods for measuring μ_r . One of them was the direct calculation of the area of dips in Fig. 1. Scattering of the values provides an estimate for the accuracy of measurement of μ_r , which is also given in the table.

If we are interested in statistical data only, as in Fig. 1, the computation of the J value after each crossing is not necessary, nor is the averaging of $J(t)$ done in [1]. This can be used to further speed up the computation by applying a simple relation $J = |p|$ at $A(t) = 0$, that is, at every second passage between crossings (see Section 2). It is especially important for the simple code in equation (2.8) that was used, and in particular, for the longest run $n = 6$ in Fig. 1. With the main standard code, this also was used for calculating two different distributions, after odd and even passages. Both are shown in Fig. 1 for $n = 1$ and 5. The total regular areas for both distributions are close to each other. Yet the positions of dips are different, sometimes significantly. Another interesting peculiarity is the concentration of a regular component near $J \approx 0.9$.

Even though the total regular area is very small ($\sim 1\%$), its local share can be as large as 20%. In spite of stability islets, the chaotic component remains connected in the whole crossing region.

The dependence $\mu_r(\epsilon)$ is weak, if any. Apparently, the measured value already is close to the asymptotic one $\mu_r(0) \approx \langle \mu_r \rangle = 0.0072$ where the average is taken over all six cases in the table.

All these peculiarities are further discussed in Section 5.

4. DIFFUSION, INSTABILITY, AND THE CRITICAL STRUCTURE

The diffusion in J was studied for a similar model in [2]. The essential difference from our mode (2.1) was the restriction of the separatrix oscillation in (2.2) by the requirement that $A(t) > 0$. In this case, the diffusive kinetics is valid in the whole crossing region. In our model, the diffusive regime is restricted to the domain $J > \epsilon^{1/3}$, while the ballistic regime takes over for $J < \epsilon^{1/3}$ with completely different kinetics (see [1] and below).

The diffusion rate in the random phase approximation (RPA) immediately follows from a simple expression for the change of J per separatrix crossing

$$\Delta J(J, \phi, \epsilon) = \mp \frac{\epsilon}{2} \frac{\sqrt{1 - J^4}}{J^2} \ln |2 \sin \phi|, \quad (4.1)$$

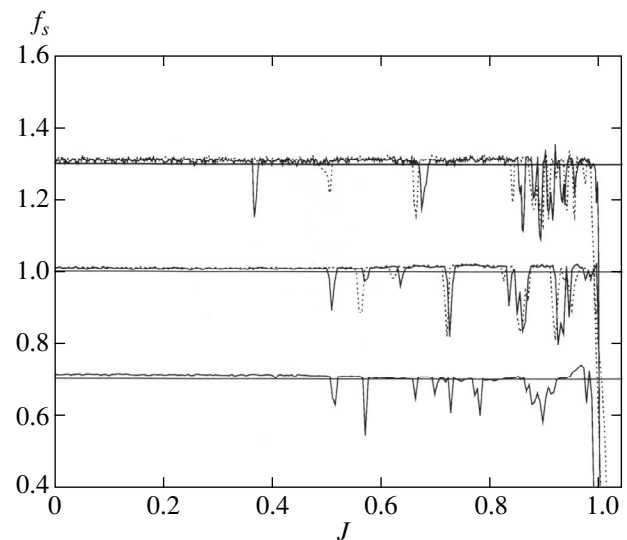


Fig. 1. Histogram of the steady-state distribution for three values of ϵ (see the table): ($n = 4$) the upper curve shifted up by 0.3; ($n = 5$) the middle curve; and ($n = 6$) the lower curve shifted down by 0.3. Solid lines correspond to J values at $|A(t)| = 1$, and the dotted ones are related to $A(t) = 0$ (see the text).

where the sign coincides with that of $\dot{A}(t)$, and is given by the relation

$$D_0 = \langle (\Delta J)^2 \rangle = \frac{\epsilon^2 \pi^2}{48} \left(\frac{1}{J^4} - 1 \right), \quad (4.2)$$

where the subscript zero indicates the RPA (see [2] and [14] therein).

The simple relation in equation (4.1) was carefully checked in [1], and proved to be surprisingly accurate in the whole diffusive region $J > \epsilon^{1/3}$. However, as was shown already in [2], the correlation-free diffusion rate (4.2) is valid for few crossings only (see also [1]). After that, the correlation in ϕ builds up, thereby decreasing the diffusion rate D by a factor of 2. We present the results of more systematic local diffusion rate measurements than in the RPA theory (4.2). To this end, we computed the correlation factor as the ratio

$$R(\langle J \rangle) = \frac{\langle D \rangle}{\langle D_0 \rangle}. \quad (4.3)$$

This was done as follows. The number of trajectories $N_{tr} = 100$ with initial value $J = J_0$ and random x were run during $T = 800$ to 1600 separatrix crossings. The empirical diffusion rate was then calculated in the standard way, as

$$\langle D \rangle = \frac{\langle (J(T) - J_0)^2 \rangle}{T}$$

with averaging over all the trajectories, while the RPA theoretical rate $\langle D_0 \rangle$ was computed by averaging

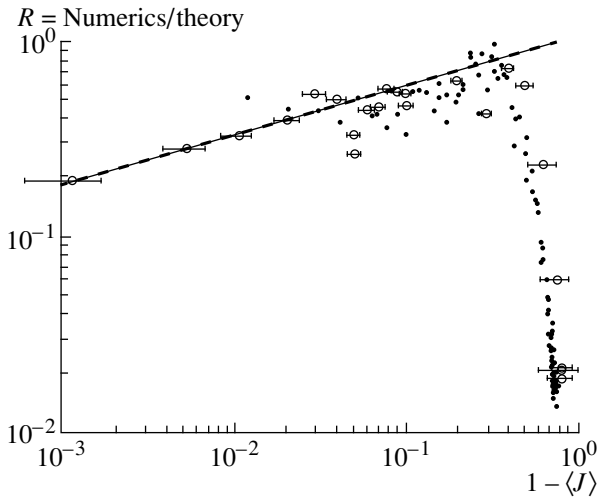


Fig. 2. The ratio of empirical to theoretical diffusion rate (the correlation factor (4.3)) vs. the mean action $\langle J \rangle$: $\epsilon = 0.001$ (circles); $\epsilon = 0.003$ (dots). Error bars show the spreading of trajectories during diffusion. The dashed straight line is fit (4.4) to four extreme left points ($\epsilon = 0.001$).

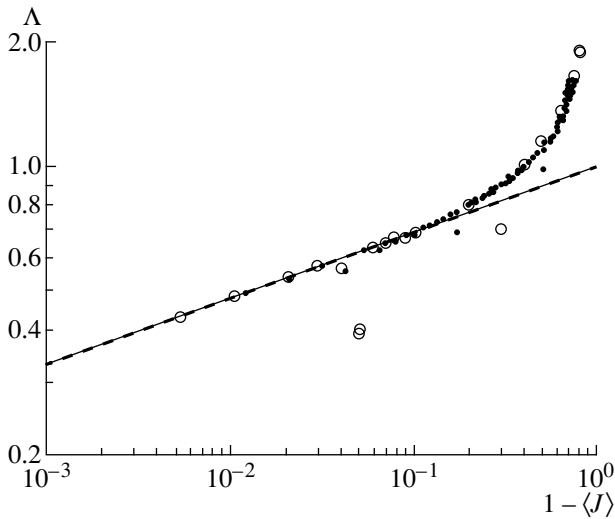


Fig. 3. The Lyapunov exponent Λ per crossing vs. mean action $\langle J \rangle$: $\epsilon = 0.001$ (circles); $\epsilon = 0.003$ (dots). The dashed straight line is fit (4.6) to ten extreme left points ($\epsilon = 0.001$).

expression (4.1) over all $N_r \times T$ crossings. Altogether, 23 groups of trajectories with different initial J_0 in the whole range $0 \leq J_0 < 1$ (and with random x) were run and related to the mean value $\langle J \rangle \neq J_0$ over all the crossings. Actually, all the $\langle J \rangle$ values were found to lie outside the ballistic domain because the trajectory quickly leaves the latter [1]. Nevertheless, for the initial value $J_0 > \epsilon^{1/3}$, the trajectory spent some time within this domain, and we needed a certain empirical relation for the “diffusion rate” to perform averaging $\langle D_0 \rangle$. This was obtained from the results of [1] in the form

$$D_0 = 0.16\epsilon^{2/3}, \quad J < \epsilon^{1/3}.$$

It depends on ϵ but not on J .

The results of these numerical experiments are presented in Fig. 2 in the log–log scale using the quantity $1 - \langle J \rangle$ rather than $\langle J \rangle$ as the argument. The reason for this is our special interest in the asymptotic regime $J \rightarrow 1$ at the chaos border in phase space on the edge of the crossing region. Typically, one would expect a very peculiar critical structure here (see, e.g., [8]). This interesting question is discussed later in this section.

We show in Fig. 2, the fit of the four extreme left points in the immediate vicinity of the chaos border to a power law expected in the critical structure. The result is

$$R(J) = 1.05(1 - J)^{0.25}. \quad (4.4)$$

It is interesting that this simple relation also describes, to a reasonable accuracy, the rest of points except the five with the smallest $\langle J \rangle$ that are affected by the ballistic regime as explained in what follows. Some clear deviations from the smooth relation (4.4) reveal a certain fine structure of the diffusion of an unknown origin.

The factor R in (4.3) is always less than one, which means there is suppression of the diffusion by the correlation. The minimal suppression (maximal R) occurs at $J = J_D \approx 5\epsilon^{1/3}$, which is much larger than the crossover to the ballistic region at $J = \epsilon^{1/3}$. This is the answer to the question about the width of the ballistic-affected region put forward in the conclusion of our previous publication [1]. For $J \leq J_D$, the correlation strongly suppresses the diffusion down to a very low rate, which is apparently determined by fluctuations. These unusual kinetics certainly deserve further study. In any event, such a suppression explains a surprisingly long-motion time required for a good steady-state distribution in Fig. 1. The value of J_D marks the diffusion crossover from a big to a small correlation (cf. Fig. 3). In the complementary region $J \geq J_D$, the correlation factor also decreases, although very slowly, see (4.4). Within fluctuations, which increase with ϵ , the factor R does not depend on ϵ (for the explanation, see Section 5).

The diffusion rate itself is given by the empirical relation

$$D(J) \approx \frac{\pi^2}{48} \epsilon^2 \frac{(1 - J^4)(1 - J)^{1/4}}{J^4} \rightarrow \frac{\pi^2}{12} \epsilon^2 (1 - J)^{c_D}, \quad (4.5)$$

where the latter expression represents the asymptotics as $J \rightarrow 1$, and $c_D \approx 5/4$ is the diffusion critical exponent.

A power law in equation (4.5) suggests the existence of a critical structure at the chaos border $J = 1$. Detailed study of this structure is hampered by some additional border effects as discussed in Section 3. Even for a rather small $\epsilon = 0.001$, we managed to follow the asymptotic behavior to $1 - J \sim 10^{-3}$ only (see Fig. 2). Also, we are not able, as yet, to calculate the critical exponent c_D from the existing resonant theory of the critical phenomena [8]. However, there is another way to test our conjecture. Namely, besides the local diffu-

sion rate, we might measure the asymptotic behavior of the Lyapunov exponent $\Lambda(J)$. In fact, we did both simultaneously in the same run.

A positive Lyapunov exponent ($\Lambda > 0$) is the main condition for the strongest statistical properties in a dynamical system, including the randomness of most trajectories [10] (see also [11, 12]). The other condition for chaos is the boundedness of motion in the phase space. The first measurement of Λ (for the same model) was reported in [13], just as a criterion for chaos. Formally, the Lyapunov exponent is defined in the ergodic theory of dynamical systems in the limit as $t \rightarrow \infty$ [7] (as is the diffusion rate, by the way). However, for rather different time scales of motion, the local Lyapunov exponent $\Lambda(J)$ also becomes a meaningful and, moreover, a very important characteristic of the motion. Roughly, the ratio of time scales is that of error bars to the corresponding J values in Fig. 2 provided the number of crossings T per trajectory is sufficiently large for Λ to saturate.

In Fig. 3, we present the results for $\Lambda(J)$ measured, as $D(J)$, per one separatrix crossing, and for the same parameters and initial conditions as in Fig. 2. A clear crossover to asymptotic behavior is seen at $\langle J \rangle = J_\Lambda \approx 0.8$. The latter was also fitted to the power law

$$\Lambda(J) = 0.98(1 - J)^{c_\Lambda}, \quad (4.6)$$

with the critical exponent $c_\Lambda = 0.156$. In fitting, we used ten extreme left points besides the two at $\langle J \rangle = 0.95$ that represent some unknown fine structure (cf. Fig. 2). Below the crossover ($J > J_\Lambda$), the dependence is approximately linear,

$$\Lambda(J) \approx 1.9 - 1.4J. \quad (4.7)$$

The fluctuations are now much less than for $D(J)$. In both cases, the ϵ -dependence, if any, is weak. Interestingly, no effect of the ballistic region is seen for $\Lambda(J)$ (cf. Fig. 2).

The theory of critical phenomena [8] allows one to calculate the ratio of the two exponents, irrespective of other details of the critical structure. The ratio is

$$r_{th} = \frac{c_D}{c_\Lambda} = 8, \quad (4.8)$$

while the empirical value for this ratio from equations (4.5) and (4.6) is $r_{exp} = 8.01$, a surprising agreement!

To illustrate this result, we plot, in Fig. 4, the dependence $D(\Lambda)/\epsilon^2$ together with the expected asymptotic relation

$$\frac{D}{\epsilon^2} = \Lambda^8. \quad (4.9)$$

This appealing result strongly suggests the existence of a critical structure at the chaos border $J = 1$, and further studies of this interesting problem are needed.

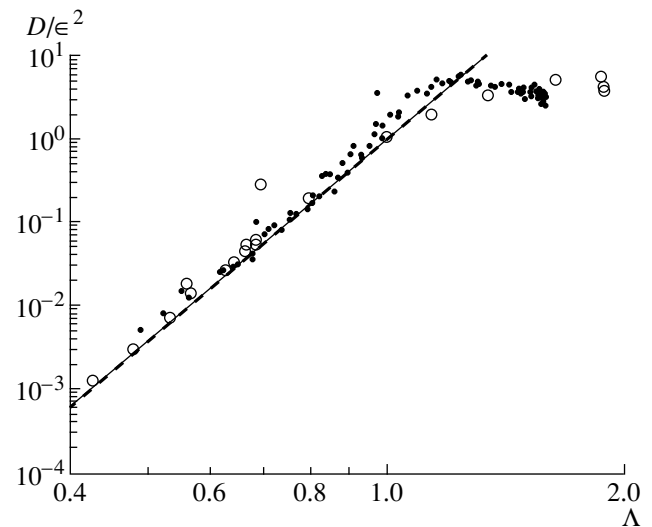


Fig. 4. Diffusion rate vs. the Lyapunov exponent: $\epsilon = 0.001$ (circles); $\epsilon = 0.003$ (dots). The dashed straight line is the theoretical prediction for the critical structure (4.9)

5. A SIMPLE MAP

Because the principal change in the adiabatic invariant J occurs at the separatrix crossing, it is natural to derive a 2D-map per crossing. These sorts of maps were considered by many authors [2, 3, 14, 15]. All these maps are rather complicated, at least for theoretical analysis. For the model under consideration here, the global map (in J) has the form

$$\bar{J} = J \mp \frac{\epsilon \sqrt{1 - J^4}}{2J^2} \ln |2 \sin \phi|, \quad (5.1)$$

$$\bar{\phi} = \phi + \Phi(\bar{J}),$$

where the sign coincides with that of $\dot{A}(t)$ (see equation (4.1)). The difficulty of constructing and using such a map lies in the second equation. Note that both equations are approximate and cannot be substitutes for the exact equations of motion even in the simplest form of another map (2.8).

To simplify the global map (5.1), we first transform it to a local one by the standard procedure, the linearization of the second equation (see, e.g., [5, 6]):

$$\Phi(J) \rightarrow \pi n + \left(\frac{d\Phi}{dJ} \right)_{J=J_n} \Delta J. \quad (5.2)$$

The new parameter J_n satisfies the equation $\Phi(J_n) = \pi n$ with any integer n , and $\Delta J = J - J_n$. In our problem, this approximation is rather accurate for sufficiently small $\epsilon \rightarrow 0$. In particular, we can consider the discrete variable J_n as a continuous one (see below).

Typically, the derivative $\Phi' = d\Phi/dJ$ is still very complicated, and we assume another principal approximation; calculating the change in ϕ between succes-

sive separatrix crossings, we use the limiting motion frequencies neglecting the change of those near the separatrix. They are

$$\begin{aligned} \omega_r &= \frac{4}{\pi} J \quad \text{for phase rotation,} \\ \omega_o &= \sqrt{A(t)} \quad \text{for phase oscillation.} \end{aligned} \tag{5.3}$$

The rotation frequency (off the resonance) remains constant between crossings, while the oscillation slowly varies due to the separatrix motion. Now, the full period of the phase ϕ , which is equal to π , corresponds to the full period of the rotation, but only to a half of that for the oscillation. Therefore, the speed of the o variation in this approximation becomes

$$\frac{d\phi}{dt} = \begin{cases} \frac{\omega_r}{2} = \frac{2}{\pi} J, & J > \sqrt{A(t)}, \\ \omega_o = \sqrt{A(t)}, & J < \sqrt{A(t)}. \end{cases} \tag{5.4}$$

The latter inequalities determine the transition from rotation to oscillation and back, which occurs at the crossing time $t = t_{cr}$ where (see equation (2.7))

$$\epsilon t_{cr} = \arcsin(J^2). \tag{5.5}$$

For the local map in question, we need only the derivatives Φ' , which are expressed in terms of elementary functions as

$$\Phi'(J) = \begin{cases} \frac{8}{\pi\epsilon} \left(\frac{1}{2} \arcsin(J^2) + \frac{J^2}{\sqrt{1-J^4}} \right), & J > \sqrt{A(t)}, \\ \frac{4}{\epsilon} \frac{J^2}{\sqrt{1-J^4}}, & J < \sqrt{A(t)}. \end{cases} \tag{5.6}$$

Since the most interesting part of the motion structure is essentially concentrated near sufficiently large $J \approx 0.9$ (see Fig. 1), we can keep in the first equation (5.6) only the second term with the coefficient $4/\epsilon$ from the second equation. In fact, the difference between the two factors is less than it appears just because of the contribution of the omitted term. However, the latter correction would be certainly an excess in accuracy for our rather crude map. Finally, we assume

$$\Phi'(J) \approx \pm \frac{4}{\epsilon} \frac{J^2}{\sqrt{1-J^4}}. \tag{5.7}$$

The local map is now derived from equations (5.1), (5.2), and (5.7) in the standard way (see, e.g., [5, 6, 16]), and has the form

$$\begin{aligned} \bar{P} &\approx P \mp K \ln|2 \sin \phi| \pmod{\pi}, \\ \bar{\phi} &\approx \phi \mp \bar{P} + \frac{\pi}{4}, \end{aligned} \tag{5.8}$$

where the signs in both equations change simultaneously at each crossing, and where

$$P = \frac{4}{\epsilon} \frac{J_n^2}{\sqrt{1-J_n^4}} \Delta J \pmod{\pi} \tag{5.9}$$

is a new, local, momentum, and the only parameter $K \approx 2$ is simply a constant in the approximation assumed. An additional phase change by $\pi/4$ comes from the shift of the separatrix by π in x each time it crosses zero (see equation (2.4)). Literally, this change in ϕ is equal to $\pi/4 \pm \pi/4$, but the alternating part simply shifts P by a constant $\pi/4$ and, thus, can be omitted.

The phase space of the local map (5.8) is a 2D-torus $\pi \times \pi$. It approximately represents a narrow strip $\Delta_1 J \times \pi$ in the phase space of our main system (2.1), where

$$\Delta_1 J = \frac{\pi\epsilon \sqrt{1-J_n^4}}{4 J_n^2}. \tag{5.10}$$

For the local map to be applicable, the following two conditions are to be satisfied:

$$\frac{\Delta_1 J}{J_n} \approx \frac{\epsilon}{J_n^3} \lesssim 1, \tag{5.11}$$

and

$$\frac{\Delta_1 J}{1-J_n} \approx \frac{\epsilon}{\sqrt{1-J_n}} \lesssim 1. \tag{5.12}$$

The latter condition excludes a very narrow domain $1 - J_n \leq \epsilon^2$, which is practically impossible to observe, while the former comprises the whole ballistic region.

The density of local strips (5.10) in J_n ,

$$\frac{dn}{dJ_n} \approx \frac{1}{\Delta_1 J} = \frac{4}{\pi\epsilon} \frac{J_n^2}{\sqrt{1-J_n^4}}, \tag{5.13}$$

is rapidly increasing with J_n , which explains the concentration of the regular component near the chaos border (Fig. 1). This also explains the shift δJ of the dips between two different groups in Fig. 1. The largest $\delta J \approx 0.15$ on the upper curve between the two extreme left dips is close to the full width of the corresponding local strip $\Delta_1 J \approx 0.16$.

An interesting feature of the 4-step map in equation (5.8) over a period of the adiabatic perturbation (four separatrix crossings) is a singularity at $\phi = 0 \pmod{\pi}$. The Fourier spectrum of this singularity

$$\ln|2 \sin \phi| = - \sum_{n=1}^{\infty} \frac{\cos(2n\phi)}{n} \tag{5.14}$$

is similar to that of the function with a finite discontinuity. As is well known (see, e.g., [8, 17] and references therein), the chaotic component of such a motion is always connected. This means that there is no invariant

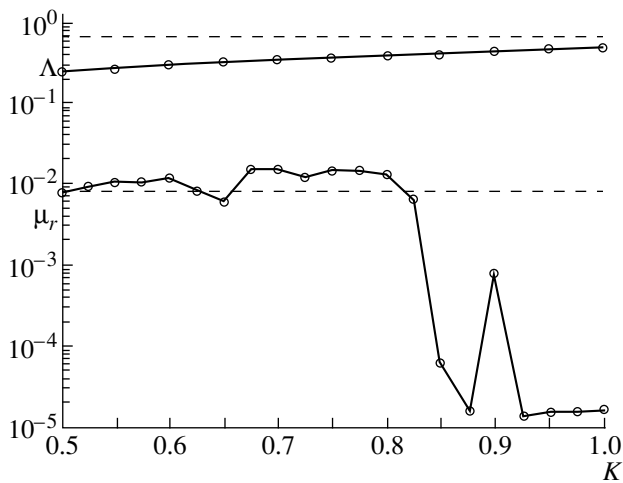


Fig. 5. Comparison of local map (5.8) (circles connected by lines to guide the eye) and the main system (2.1) (dashed lines) with respect to: the relative measure μ_r of the regular component (lower data), and the Lyapunov exponent Λ (upper data). For the main system, the dashed lines give $\mu_r = 0.007$ and $\Lambda (J = 0.9) = 0.67$ (see the text).

curve in the entire range $0 \leq \phi \leq \pi$ that would cut through and disconnect the chaotic component.

This confirms earlier conjectures on the universality of chaos under the separatrix crossings (see, e.g., [13]). The motion in such a system is typically nonergodic, that is, it contains a regular component. For a particular model under consideration, it was first found in [3], and studied in detail in the present work (Section 3). Using a simple map in equation (5.8), we are able to analyze and understand particular features of this less-known component of the motion.

To this end, we first measured the relative area μ_r of the regular component (stability islets) within the local phase-space cell ($\pi \times \pi$) as a function of the parameter K . The result is shown in Fig. 5 (lower circles). In the approximation of a constant parameter K , the relative area is the same in each cell, and thus, is approximately equal to the relative area in the whole range of J in the main system. The latter is also shown in Fig. 5 (the lower dashed line). The agreement, within a factor of 2, seems reasonable provided the local parameter is $K \leq 0.8$, which is about half of the estimated value. Assuming $K \approx 0.8$, we can further compare the Lyapunov exponent in the local map (upper circles in Fig. 5) with that of the main system at $J = 0.9$, the latter being larger by a factor of 2 (the upper dashed line).

Besides a qualitative description, therefore, a simple local map (5.8) leads to quantitative estimates within a factor of 2, which is not that bad for such a primitive map.

The local map is independent of ϵ , and so are all the dimensionless quantities of the variables and the parameters of this map. These include the relative area μ_r (cf. Fig. 1 and the table), the Lyapunov exponent Λ

per separatrix crossing (or per perturbation period) (Fig. 3), and the correlation factor R (Fig. 2) except for small J close to the ballistic region, where the local map is not applicable.

6. CONCLUSION

We studied the structure and statistical properties of the chaotic motion under the separatrix crossing in numerical experiments with a typical model (2.1) used in such studies. An interesting distinction from the previous studies (except [13]) is in that we allow the full swing of the separatrix ($-1 \leq A(t) \leq 1$). In this case, the chaos comprises the whole range ($0 \leq J \leq 1$), and there is only one chaos border at $J = 1$. Usually, the perturbation amplitude $A(t) > 0$ is strictly positive (or negative) which implies two chaos borders with the chaotic component between them ($0 < J_1 \leq J \leq 1$), but without an interesting ballistic region.

We have qualitatively confirmed the previous results on the existence of the regular component (nonergodicity) of motion [3] and the correlation in the chaotic component suppressing the diffusion [2]; we have found many other interesting details of the motion structure (Sections 3 and 4). For a physical interpretation and understanding of our empirical results, we have constructed a very simple but meaningful local map per separatrix crossing, which leads not merely to a qualitative description of the chaos structure, but also to a reasonable quantitative estimates within a factor of 2.

In Fig. 1, most of the regular component is seen near the chaos border, at $J \approx 0.9$. We never observed any at $J = 0$, which is at variance with the prediction in [14] based on approximating the equations of motion by the Mathieu equation at small $\epsilon \rightarrow 0$. The resolution of this apparent contradiction is that the parametric perturbation amplitude in the Mathieu equation increases as $\propto \epsilon^{-2}$ (see equation (2.9)), and therefore, stable periodic solutions are only possible in special very narrow windows of ϵ . An interesting open question is the size of the corresponding stability islets.

Another interesting problem is the expected critical structure at the chaos border $J = 1$. The standard method—statistics of the Poincaré recurrences (see, e.g., [8] and references therein)—is difficult to apply here because of the confusion with many internal chaos borders around stability islets of the regular component. Instead, we measured the $J \rightarrow 1$ asymptotic behavior of the two quantities, $\Lambda(J)$ and $R(J)$. Unfortunately, we were not able to calculate from the existing theory [8] the two critical exponents separately, because of the singularity at $J = 1$ (see equation (5.6)). However, we have found that their ratio (4.8) is independent of the singularity and agrees surprisingly well with the empirical result (Fig. 4). This is strong evidence in favor of the critical structure, and it certainly deserves further studies.

In the present work, as well as in the previous one [1], we studied the crossing of a single separatrix that is one of the two separatrix branches of a nonlinear resonance (see equation (2.1)). As is well known, there is another, related but not identical, process, the crossing of the whole resonance with both of its branches. The latter was studied even much earlier [18] (see also [19]). From the beginning, it was found that the change in the adiabatic invariant per crossing, $\Delta J \sim \epsilon \ln \epsilon$ (in dimensionless variables), differs from that for the separatrix crossing, calculated much later, by an additional factor $\ln \epsilon$, which slowly but indefinitely grows as $\epsilon \rightarrow 0$. The importance of this factor for the regular component of the motion was understood in [3]. Namely, it was theoretically predicted that the stable trajectories of the two particular periods are destroyed, together with the surrounding islets, for sufficiently small ϵ . An interesting open question is whether the whole regular component, containing infinitely many islets [8], also vanishes, and if so, then how fast.

In terms of our local map (5.8), the additional factor would completely change all the underlying motion structure because now the map parameter $K \sim |\ln \epsilon| \rightarrow \infty$ does depend on the adiabaticity parameter, and moreover, indefinitely grows as $\epsilon \rightarrow 0$. This implies the ϵ -dependence of all the dimensionless characteristics of the motion, in particular, the measure of regular component. We performed some preliminary numerical experiments to estimate the dependence $\mu_r(K)$. Asymptotically, it looks like an exponential, which would imply a power law for $\mu_r(\epsilon)$.

In the very conclusion, we would like to mention that the latter particular interesting question is a part of a very important and very difficult unsolved general problem in the theory of dynamical systems, the problem of ergodicity in the case of analytic or even sufficiently smooth equations of motion.

ACKNOWLEDGMENTS

This work was partially supported by the Russian Foundation for Basic Research (grant no. 97-01-00865).

REFERENCES

1. B. V. Chirikov and V. V. Vecheslavov, Preprint No. 99-52 IYaF SO RAN (Budker Institute of Nuclear Physics, Siberian Division, Russian Academy of Sciences, Novosibirsk, 1999); Zh. Éksp. Teor. Fiz. **117**, 644 (2000) [JETP **90**, 562 (2000)].
2. D. Bruhwiler and J. Cary, Physica D (Amsterdam) **40**, 265 (1989).
3. A. I. Neishtadt, V. V. Sidorenko, and D. V. Treschev, Chaos **7**, 2 (1997).
4. B. Mirbach and G. Casati, Phys. Rev. Lett. **83**, 1327 (1999).
5. B. V. Chirikov, Phys. Rep. **52**, 263 (1979).
6. A. Lichtenberg and M. Leiberman, *Regular and Chaotic Dynamics* (Springer, New York, 1992).
7. I. Cornfeld, S. Fomin, and Ya. Sinai, *Ergodic Theory* (Springer, New York, 1982).
8. B. V. Chirikov, Chaos, Solitons and Fractals **1**, 79 (1991).
9. Y. Elskens and F. Escande, Nonlinearity **4**, 615 (1991); Physica D (Amsterdam) **62**, 66 (1993).
10. V. M. Alekseev and M. V. Yakobson, Phys. Rep. **75**, 287 (1981).
11. B. V. Chirikov, Open Systems & Information Dynamics **4**, 241 (1997).
12. B. V. Chirikov and F. Vivaldi, Physica D (Amsterdam) **129**, 223 (1999).
13. C. Menyuk, Phys. Rev. A **31**, 3282 (1985).
14. F. Escande, in *Plasma Theory and Nonlinear and Turbulent Processes in Physics*, Ed. by V. G. Baryakhtar, V. M. Chernousenko, N. S. Erokhin, A. G. Sitenko, and V. E. Zakharov (World Scientific, Singapore, 1988), p. 398.
15. J. Cary and R. Skodje, Phys. Rev. Lett. **61**, 1795 (1988); Physica D (Amsterdam) **36**, 287 (1989).
16. B. V. Chirikov, in *Reviews of Plasma Physics*, Ed. by B. B. Kadomtsev (Énergoatomizdat, Moscow, 1984; Consultants Bureau, New York, 1987), Vol. 13.
17. I. Dana, N. Murray, and I. Percival, Phys. Rev. Lett. **62**, 233 (1989).
18. B. V. Chirikov, Dokl. Akad. Nauk SSSR **125**, 1015 (1959) [Sov. Phys. Dokl. **4**, 390 (1959)]; B. V. Chirikov and D. L. Shepelyansky, Zh. Tekh. Fiz. **52**, 238 (1982) [Sov. Phys. Tech. Phys. **27**, 156 (1982)].
19. J. Cary, F. Escande, and J. Tennyson, Phys. Rev. A **34**, 4256 (1986).